Journal of Building Engineering 25 (2019) 100791

Contents lists available at ScienceDirect

Journal of Building Engineering

journal homepage: www.elsevier.com/locate/jobe

# Performance of sustainable high strength concrete with basic oxygen steel-making (BOS) slag and nano-silica

Seyed Alireza Zareei[a,*], Farshad Ameri[b], Nasrollah Bahrami[a], Parham Shoaei[c], Hamid Reza Moosaei[a], Niloofar Salemi[a]

[a] Department of Civil Engineering, Isfahan (Khorasgan) Branch, Islamic Azad University, Isfahan, Iran
[b] Young Researchers and Elite Club, Isfahan (Khorasgan) Branch, Islamic Azad University, Isfahan, Iran
[c] Department of Civil Engineering, Sharif University of Technology, Tehran, Iran

ARTICLE INFO

*Keywords:*
High strength concrete (HSC)
Basic oxygen steel-making (BOS) slag
Nano-silica
Mechanical properties
Durability

ABSTRACT

This study presents the results of an experimental evaluation of the performance of high strength concrete (HSC) with basic oxygen steel-making (BOS) slag and nano-silica respectively used as a partial replacement of sand and cement. The properties of fresh and hardened concrete specimens containing 25%, 50%, 75%, and 100% BOS as partial replacement of sand and 2% of cement replaced with nano-silica were evaluated. According to the results, concrete samples containing nano-silica with higher BOS percentages, demonstrated improvements in strength and durability properties, while workability was reduced. For example, at 50% BOS content, about 18% increase in compressive strength and 50% reduction in water absorption was observed, while slump was reduced by 40%.

## 1. Introduction

Concrete is one of the most widely used construction materials in all around the world due to its ease of access, durability, and proper mechanical properties. The global concrete consumption is estimated about 25 billion tons yearly. The large consumption volume of this construction material has raised many environmental issues including depletion of natural raw materials, problems associated with extraction of natural sand from river beds [1], and a great decrease in resources of fine aggregates in the past 15 years [2]. Furthermore, the greenhouse effect caused by ordinary Portland cement (OPC) production is the main source of $CO_2$ emissions [3], being responsible for 5–7% of global $CO_2$ emissions [4].

These problems have led many researchers to investigate alternative materials for partial or full replacement of natural aggregates or cement to reduce environmental impacts [5]. One alternative is to replace fine aggregates with some by-products, which can be categorized as: 1) agricultural such as rice husk ash [6,7], 2) industrial such as fly ash [8–11], cement kiln dust [12], silica fume [13], granulated blast furnace slag (GBFS) [5], and bagasse ash [14], and 3) municipal wastes including glass, plastics [15], and paper [16]. Rashad provided a general review on using different types of wastes in mortar and concrete [17].

Regarding the industrial wastes, steel-making slag, especially Basic Oxygen Steel-making (BOS) slag, which is produced during the iron/steel manufacturing process, has attracted the attention of researchers due to its environmentally safe applications [18]. BOS is a non-metallic ceramic material produced from the reaction between flux such as calcium oxide and inorganic non-metallic components in the steel scrap. Typically, 130–200 kg of slag is obtained from one ton of steel depending on the composition and manufacturing process [19]. BOS slag usually contains large clusters, coarse and very fine particles [20,21]. Water is typically poured over slag as it is channeled out of the furnace, providing rapid cooling. This process causes a series of chemical reactions to occur within the slag and causes the material to behave similar to rocks. The chemical composition of slag depends on furnace type, steel grades, and pretreatment method, but generally it consists of $SiO_2$, CaO, $Fe_2O_3$, FeO, $Al_2O_3$, MgO, MnO, and $P_2O_5$ [22]. Furthermore, the grind ability index of steel slag is 0.7, compared to the value of 0.96 and 1.0 for blast furnace slag and standard sand, respectively [23].

The advantageous features of BOS such as simple manufacturing process and long term stability in unbound conditions have made it as an appropriate alternative granular material in concrete manufacturing [24]. Maslehuddin et al. [25], reported that concrete containing steel slag as partial replacement of cement shows higher mechanical and durability properties. Wen et al. [26], reported that concrete with steel slag exhibits higher compressive strength and an excellent anti-chloride

* Corresponding author.
*E-mail address:* a.r.zareei@khuisf.ac.ir (S.A. Zareei).

https://doi.org/10.1016/j.jobe.2019.100791
Received 5 October 2018; Received in revised form 22 March 2019; Accepted 28 April 2019
Available online 08 May 2019

ion penetration performance. Subathra and Gnanavel [27] studied recyclable ground granulated blast furnace slag (GGBFS) materials, as partial replacement of sand with percentages of 10%, 20%, 30%, 40%, and 50%. The maximum compressive strength was observed in mix designs with 50% GGBFS content. Furthermore, it was reported that further replacement levels led to reduced compressive strength [27,28]. Kuthai and Malathy [29] studied the effect of steel slag on mechanical properties of concrete. They reported that mix designs with 30% steel slag exhibited improved compressive strength, flexural strength, and modulus of elasticity. Manjunath and Narasimhan [30] used steel slag as fine aggregates to produce self-compacting alkali-activated slag concrete. Results showed that incorporation of steel slag improved the compressive strength and reduced water absorption.

Furthermore, some studies investigated the possibility of using nano-silica in different concrete types. Aydın et al. [31] studied the behavior of self-compacting concrete with nano-silica and carbon nano tubes combined with different percentages of fly ash. It was shown that concrete with 2% nano-silica, 0.08% carbon nano tubes, and 40% fly ash exhibited the best performance. Naniz and Mazloom [32] studied the influence of different levels of nano-silica on fresh and hardened properties of self-compacting concrete with different water-to-binder ratios. According to the experimental results, replacing 3% of cement with nano-silica led to satisfactory self-compacting concrete. Mohammed and Adamu [33] examined the performance of roller compacted concrete pavement with 1%, 2%, and 3% nano-silica as replacement of cement with different crumb rubber levels. The results showed improved microstructure, strength, and durability.

In the light of previous studies, the main objective of the present experimental work was to investigate the feasibility of producing high strength concrete (HSC) containing BOS and nano-silica as partial replacement of natural fine aggregates and cement, respectively. As far as the authors are concerned, no study to date has evaluated the mechanical properties of high strength concrete containing different percentages of BOS and nano-silica at different ages. For this purpose, natural sand was partially replaced with BOS at levels of 0%, 25%, 50%, 75% and 100% by weight of sand and 2% of cement was replaced with nano-silica. The physical, mechanical, and durability properties of specimens including density, water absorption, crack width, compressive strength, tensile strength, flexural strength, modulus of elasticity, and ultrasonic pulse velocity (UPV). The experimental program in this study was designed to provide comprehensive data regarding the properties of high strength concrete with BOS and nano-silica and to contribute to better understanding of the behavior in short term and long term conditions.

## 2. Experimental program

### 2.1. Materials

#### 2.1.1. Cement

Type I cement was provided from Ardestan cement plant with specific density of 3.19 g/cm$^3$, Blaine surface area of 3050 cm$^2$/g, and 28-day compressive strength of 37 MPa. The chemical analysis of cement revealed that it is composed of 63.1% CaO, 22.5% $SiO_2$, and 6% $Al_2O_3$ followed by small amounts of MgO, $K_2O$, and $SO_3$.

#### 2.1.2. Basic oxygen steel-making (BOS) slag

BOS used in this study (see Fig. 1(a)) was provided from Mobarakeh steel plant in Isfahan, Iran (see Fig. 1(b)), with the specific gravity of 3.45 g/cm$^3$, unit weight of 1800 kg/m$^3$, and water absorption of 3%. The quality of BOS was evaluated in accordance with standard test methods including weight loss in mixtures exposed to sodium sulfate solution per AASHTO T-104 [34], weight loss ratio in Los Angeles abrasion test according to AASHTO T-96 [35], and damage percentage in 1 and 2 sides of the specimen per ASTM D-5821 [36]. The results are presented in Table 1.

Furthermore, according to the chemical analysis results, BOS particles mainly consist of calcium oxide (CaO:45%), Iron oxide (FeO:26%), Quartz ($SiO_2$:15%), and Periclase (MgO:8%). The X-ray diffraction (XRD) analysis of BOS particles also confirmed the results obtained by the chemical analysis as shown in Fig. 2. Furthermore, SEM analysis was carried out on BOS particles to gain an understanding regarding their shape and physical property. As illustrated in Fig. 3, the particles vary in size and shape and are mostly angular.

#### 2.1.3. Nano-silica

Nano-materials such as nano-silica and nano-fibers, owing to their high silica content can be used in concrete to produce additional calcium silicate hydrate (CSH) by reacting with calcium hydroxide to achieve improved strength, density, durability. Yu et al. suggested nano-silica and hybrid fibers such as steel for crack reduction and improvement of flexural strength of ultra-high performance concrete [37]. The nano-silica used in this study was provided from Isatis nano-silica industries with density of 1.4 g/cm$^3$ and PH of 9.5.

#### 2.1.4. Aggregates

.River washed gravel with 4.75–10 mm grain size and natural sand with grain size less than 4.75 mm were used as coarse and fine aggregates, respectively. The sieve analysis of gravel and sand aggregates are plotted in Fig. 4 in accordance with ASTM C33 [38].

#### 2.1.5. Super-plasticizer

Brown modified polycarboxylic ether (PCE) polymer, with specified weight of 1.06 of g/cm$^3$ And PH of 8 was incorporated as super-plasticizer in all mixes to improve workability of concrete.

### 2.2. Mix design

To investigate the effects of BOS and nano-silica on physical, mechanical, and durability properties of high strength concrete, mixtures with 25%, 50%, 75%, and 100% BOS as substitution of natural fine aggregates and a mixture containing 2% nano-silica as replacement of cement in addition to a control concrete were prepared as given in Table 2. The dosages for BOS were selected to investigate the effect of partial to full replacement of natural fine aggregates on the properties of high strength concrete. Furthermore, the percentage of nano-silica to replace cement was selected based on the values suggested by the previous studies [33,39–41]. Note that the water-to-binder ratio was fixed at 0.37 for all mixtures to strike a balance between workability and strength of the high strength concrete in consistence with previous studies [42–44]. It should be noted that the calculated amount of cement to be used in the concrete mix design was 459 kg, which was reduced to 450 kg when 2% nano-silica was included.

After casting the specimens, they were kept for 24 h in the molds and then they were demolded and immersed in water at 23 °C to be cured until the required age in accordance with IS 10086 [45].

### 2.3. Methods

The properties of fresh and hardened concrete containing different percentages of BOS were evaluated through a comprehensive experimental program. The fresh concrete workability was assessed by slump test conducted in accordance with ASTM C143/C143M − 12 [46]. Furthermore, fresh, dry, and saturated surface dry (SSD) densities were evaluated based on provisions of ASTM C138/C138M − 14 [47], ASTM C642-13 [48], and ASTM D7172–14 [49], respectively.

The compression test was conducted on cube specimens with the dimensions of 150 × 150 × 150 mm at the ages of 7, 28, and 91 days in accordance with ASTM C39/C39M–14 [50]. The splitting tensile strength of 150 × 300 mm cylindrical specimens and flexural strength of 100 × 100 × 500 mm beam specimens were determined at the ages of 7, 28, and 91 days based on ASTM C496/C496M–11 [51] and ASTM

(a) (b)

**Fig. 1.** (a) BOS used in this study, (b) Landfills of steel slag wastes in steel plant.

**Table 1**
BOS properties according to standard test methods.

| Test | Standard specification | Test result |
|---|---|---|
| Los Angeles abrasion | AASHTO T-96 [35] | 15% |
| Weight loss due to Sulfate solution exposure | AASHTO T-104 [34] | 0.25% |
| Failure in side 1 | ASTM D-5821 [36] | 99% |
| Failure in side 2 | ASTM D-5821 [36] | 96.3% |

C78/C78M–10 [52], respectively. Furthermore, the modulus of elasticity of 150 × 300 mm cylindrical specimens was evaluated according to ASTM C469/C469M–14 [53].

Regarding the durability assessment of BOS concrete with nano-silica, water absorption, surface crack width, and ultrasonic pulse velocity tests were conducted on 150 × 150 × 150 mm cube specimens in accordance with ASTM C642-13 [48], ASTM E2899–15 [54], and ASTM C597 [55], respectively. The results of the experiments are presented in the following.

## 3. Results and discussion

### 3.1. Fresh concrete

The fresh concrete workability was assessed using slump test. As observed in Fig. 5, with increasing values of BOS and inclusion of nano-silica, the slump value decreased, i.e., the control mix demonstrated the highest slump. It was observed that with inclusion of nano-silica, about 8% reduction in slump value occurred due to the increased surface area of the total binder in the mixture. Further, increase in BOS content resulted in a significant reduction of slump. For example, 61% reduction was observed in the slump value of concrete containing 75% BOS compared to the control specimen. The reduction can be attributed to the fact that BOS particles were much finer than sand, which resulted in higher surface area. Therefore, workability decreased as also reported by Kim et al. [56]. In addition, BOS particles were more angular, which increased the interlocking in the concrete mixtures and hence, workability decreased.

### 3.2. Density

Fresh, dry, and saturated surface dry (SSD) densities were measured for all mixtures. Fig. 6 shows the variations of the specimen densities with respect to BOS content. As seen, due to the higher density of BOS particles compared to natural sand, the density of concrete samples increased with increasing values of BOS, e.g., at 50% BOS, dry density increased up to 6%. Furthermore, the formation of additional CSH gel due to the reactions between nano-silica particles and hydration products, led to a denser structure and increased the dry and SSD densities.

### 3.3. Mechanical properties

#### 3.3.1. Compressive strength

The compression test was conducted on cubic samples with the side length of 150 mm at the ages of 7, 28, and 91 days. Based on the test results, inclusion of BOS and nano-silica had a positive effect on the compressive strength. Fig. 7(a) and Fig. 7(b) respectively illustrate the compressive strength and its variations for different BOS percentages at different ages. As seen, with increasing values of BOS content an ascending trend was observed. For example, by replacing 75% of sand with BOS, approximately 22%, 20%, and 21.5% increase in compressive strength at the ages of 7, 28, and 91 days compared to the control sample was observed, respectively. Furthermore, it was observed that the effect BOS on compressive strength was more pronounced at earlier

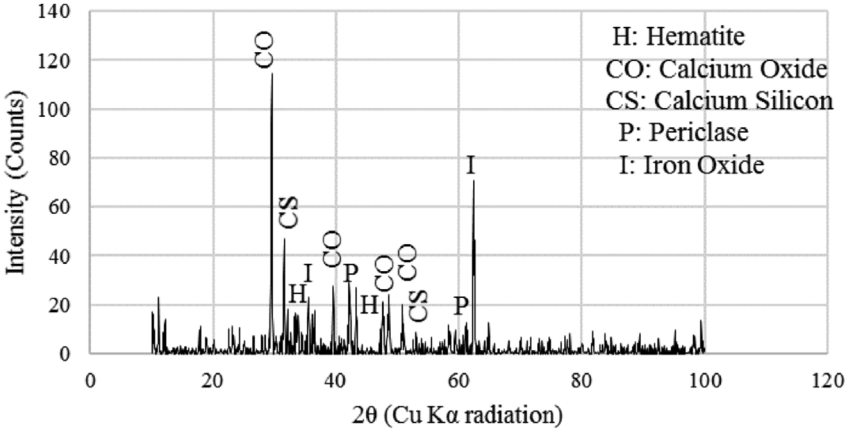


**Fig. 2.** X-ray diffraction analysis of BOS particles.

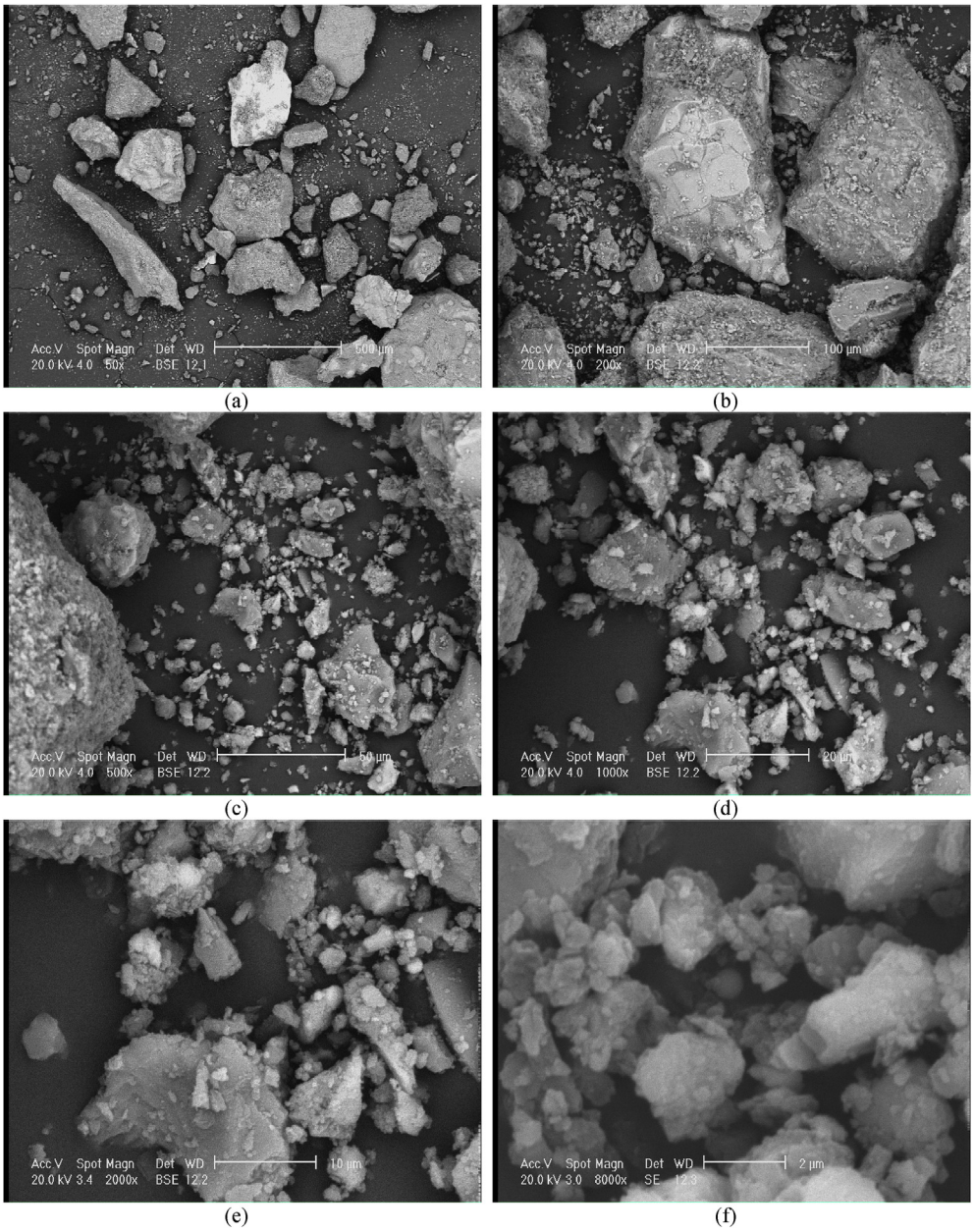


**Fig. 3.** SEM micrograph of BOS particles: (a) 50× magnification, (b) 200× magnification, (c) 500× magnification, (d) 1000× magnification, (e) 2000× magnification, (f) 8000× magnification.

ages. This was because of the chemical reactions due to the presence of free lime (about 40–50% in slag), and nano-silica as a pozzolanic material, which increased the amount of CSH gel in the concrete [57–59]. Also, inclusion of BOS and nano-silica densified the matrix and reduced the pore size due to the increased surface area of binder, which led to lower water bleeding in the interfacial transition zone as well. In addition, since the BOS particles were in angular shape, the interlocking and adhesion between the aggregates and cement paste was enhanced as also reported by [60]. The results were in a good agreement with the previous studies, which also stated that inclusion of slag as partial replacement of natural sand at levels of 5–15% led to an increased compressive strength of concrete pipes [61]. In another study, Sharmila and Dhinakaran [42] suggested 10% of ultrafine slag as the optimum value to increase strength and durability properties of high strength concrete. Qasrawi [62] reported up to 20% increase in the compressive strength of concrete with steel slag.

### 3.3.2. Splitting tensile strength

Fig. 8(a) and Fig. 8(b) show the effect of BOS on splitting tensile strength and its variations. As seen, by replacing cement with nano-silica, the splitting tensile strength was increased, e.g., 13.7%, 9.4%, and 9.8% increase in 7-, 28-, and 91-day splitting tensile strength was observed. This owed to the fact that nano-silica contains a high amount of $SiO_2$, which can react with the hydration products and produce additional CSH gel.

Furthermore, with increasing values of BOS content, an increase in the splitting tensile strength was observed. By way of illustration, by replacing natural sand with 100% BOS, 27.4%, 21.3%, and 24.5% increase in splitting tensile strength at the ages of 7, 28, and 91 days was observed, respectively. This behavior could be related to the chemical reactions between nano-silica particles and free lime existing in BOS, which yield to the production of CSH gel. Moreover, slag exhibits a pozzolanic effect in presence of calcium hydroxide $Ca(OH)_2$ [63]. The results confirmed the findings of other studies. Sharma et al. [64]

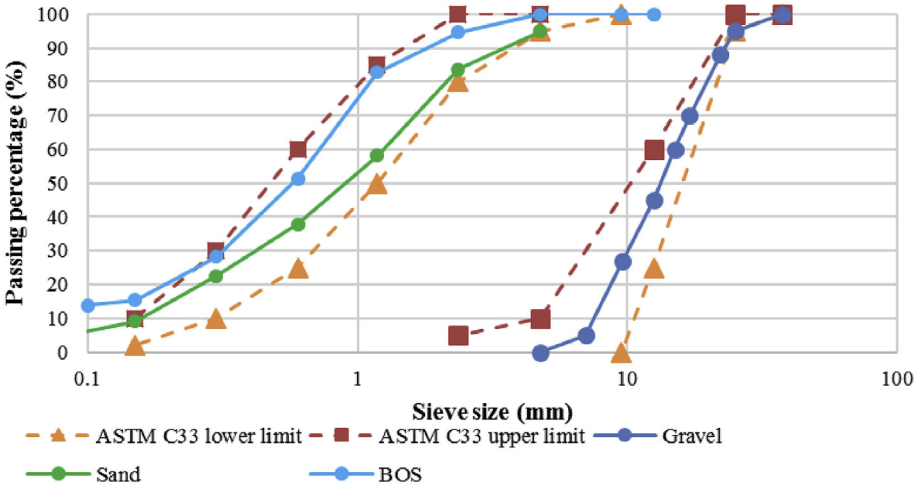


**Fig. 4.** Grain size distribution of gravel, sand, and BOS.

studied HSC with 10–50% foundry Slag (FD) as partial replacement of conventional fine aggregates and 15% alccofine as partial replacement of cement and reported improvements in compressive strength, tensile strength, and flexural strength at the ages of 7, 14, 28 and 91 days. Singh and Siddique [65] reported that self-consolidating concrete (SCC) with 40% of its fine aggregates replaced with steel slag, showed 21% higher splitting tensile strength compared to the control sample.

### 3.3.3. Flexural strength

Fig. 9(a) and Fig. 9(b) show the flexural strength of samples and its variations at the ages of 7, 28, and 91 days. Similar to the results of compression and tensile tests, replacing cement with nano-silica led to an improvement in flexural strength. For example, about 11%, 9.5% and 8.5% increase was observed. Moreover, with increasing BOS content, the flexural strength increased as well. For example, 21.4%, 19.3% and 22.6% improvement was observed in 7-, 28-, and 91-day flexural strength of specimens containing 100% BOS as replacement of sand, respectively.

As mentioned in the previous sections, two factors contributed to the strength development of concrete specimens: pore refinement by slag and nano-silica particles and production of additional CSH gel due to pozzolanic activity of BOS and nano-silica [66]. The results obtained in this study were comparable with the previous works. Singh and Siddique [65] showed that replacement of cement with steel slag improved the flexural strength, e.g., 15% increase was observed at 40% steel slag content. Also, Qasrawi [62] reported that concrete with steel slag showed improved flexural strength.

### 3.3.4. Modulus of elasticity

In general, safety, durability, density, and service life of reinforced concrete are influenced by the modulus of elasticity. Fig. 10 shows the effect of BOS and nano-silica on modulus of elasticity of concrete specimens. The average modulus of elasticity of different mixes were 45.7, 46.9, and 48 GPa when 25%, 50%, and 75% of sand was replaced with BOS. The incorporation of BOS led to increased modulus of elasticity

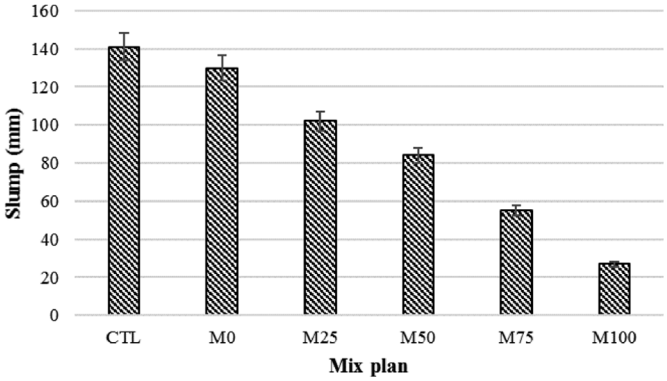


**Fig. 5.** Slump test results.

due to densification and refinement of the pore structure. The results of other studies confirmed the findings of this study. Etxeberria et al. [67] used electric arc furnace slag (EAFS) and blast furnace slag (BSF) as substitution of coarse aggregates in 25%, 50% and 100% percentages, which led to similar modulus of elasticity obtained with sand replaced by BOS in this study. Also, Singh and Siddique [65] observed a linear increase in the value of modulus of elasticity with increasing steel slag content.

### 3.3.5. Linear regression analysis

This section briefly summarizes the results of a linear regression analysis carried out on the tests data. The relationship between modulus of elasticity, flexural, tensile, and compressive strengths are presented in Fig. 11. As seen, good correlation exists between the obtained results and the high R-factor value confirms the accuracy of the proposed equations. The linear regression equations presented in this figure can be used to predict the each strength property based on the value of another.

**Table 2**
Concrete mix design.

| Mix plan | w/b | BOS (%) | BOS (kg/m$^3$) | Cement (kg/m$^3$) | Water (kg/m$^3$) | Nano-Silica (%) | Gravel (kg/m$^3$) | Sand (kg/m$^3$) | Super-plasticizer (%) |
|---|---|---|---|---|---|---|---|---|---|
| CTL | 0.37 | 0 | 0 | 450 | 170 | 0 | 900 | 750 | 0 |
| M0 | 0.37 | 0 | 0 | 450 | 170 | 2 | 900 | 750 | 1 |
| M25 | 0.37 | 25 | 187.5 | 450 | 170 | 2 | 900 | 562.5 | 1.5 |
| M50 | 0.37 | 50 | 375 | 450 | 170 | 2 | 900 | 375 | 2 |
| M75 | 0.37 | 75 | 562.5 | 450 | 170 | 2 | 900 | 187.5 | 2.5 |
| M100 | 0.37 | 100 | 750 | 450 | 170 | 2 | 900 | 0 | 3 |

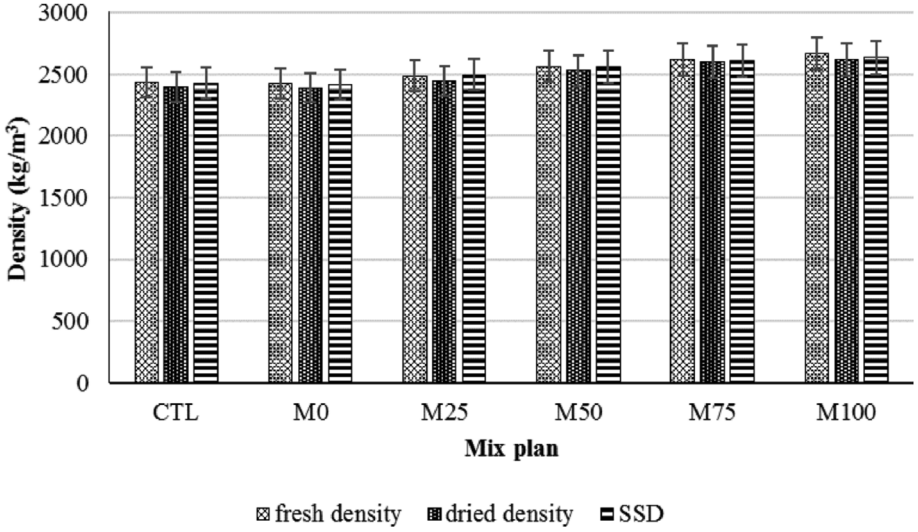


**Fig. 6.** Effects of BOS on fresh, dry, and saturated surface dry (SSD) densities.

### 3.4. Prediction of mechanical properties based on codes

Design codes and standards have proposed equations to predict the elastic modulus $E_c$, flexural strength ($f_r$), and splitting tensile strength ($f_{st}$) of concrete based on compressive strength ($f_c$) or characteristic compressive strength ($f_{cm}$) [68–73]. Generally, the experimental results should be in good agreement with the existing codes predictions. In this section, modulus of elasticity, flexural strength, and splitting tensile strength were calculated using the equations proposed by standard codes and were compared with the experimental results. To estimate the tensile and flexural strengths, different expressions have been suggested by the codes, which are listed in Table 3.

Fig. 12 compares the predicted modulus of elasticity using equations proposed by the codes to the values obtained through experiment. As seen, ACI 318, JCI-08, and ABA equations provided the closest values to the experimental ones. It seems that the expression $E_c = 5\sqrt{f'_c}$ proposed by ABA for ordinary concrete can be extended to high strength concrete. Furthermore, NZS 3101 underestimated the modulus of elasticity and the difference between the predicted and experimental values was about 20%.

Fig. 13 shows the experimental splitting tensile strength values versus the predicted ones. As observed, ACI 318 provided the closest prediction, while JSCE-07 and NZS 3101 underestimated the splitting tensile strength. On the other hand, EC-04 and JCI-08 overestimated the splitting tensile strength about 26% by average.

Moreover, Fig. 14 demonstrates the results regarding flexural strength. As seen, all design codes except EC-04, provided comparable predictions. Flexural strength predicted by ACI 318 was closest to the experimental data with the maximum difference of 5%. In addition, EC-04 provided overestimated predictions up to 50%. In summary, the equations proposed by ACI 318 led to the best prediction of the mechanical properties with reference to the experimental data.

### 3.5. Durability properties

#### 3.5.1. Water absorption

The water absorption of concrete with different BOS percentages were determined using the following relationship:

$$W_i = 100 \times \frac{W_w - W_D}{W_D} \quad (1)$$

In which, $W_i$ denotes water absorption at 30 min, $W_D$ is the dried

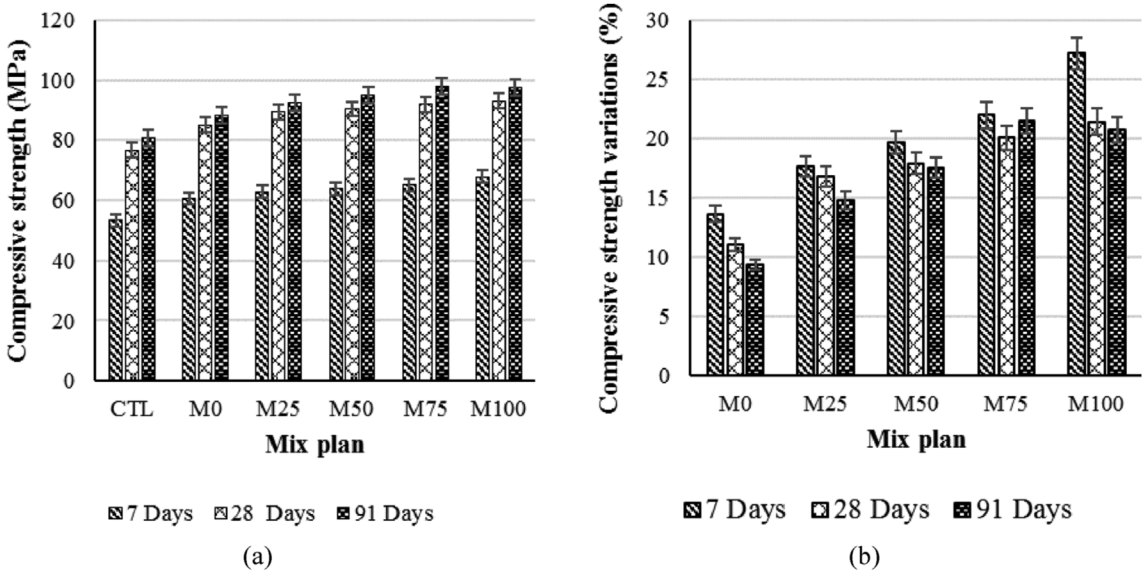


**Fig. 7.** (a) Compressive strength of different concrete mixtures at different ages, (b) Compressive strength variations.

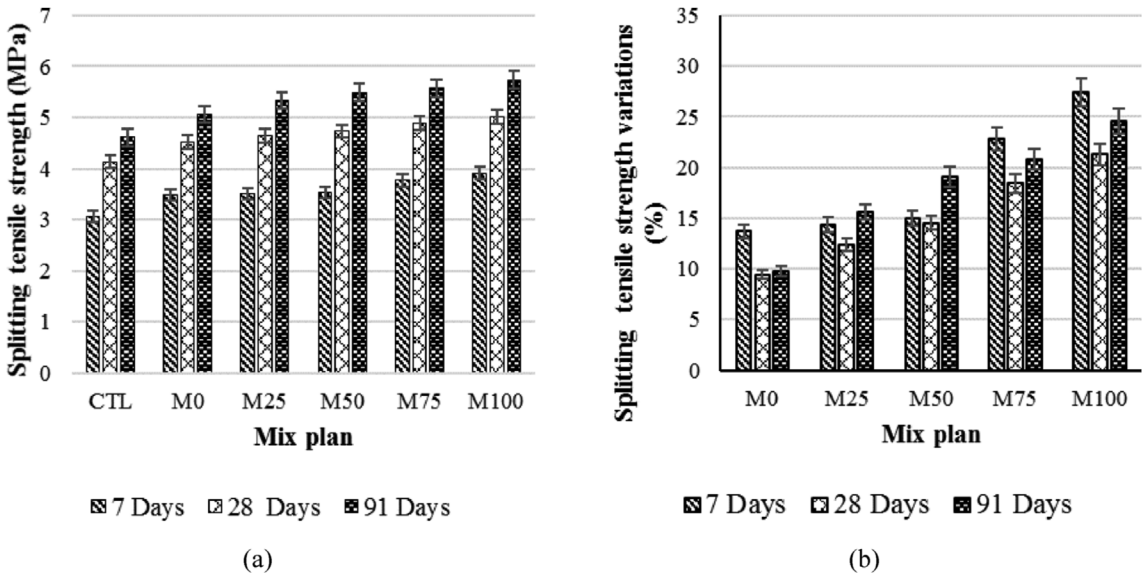


**Fig. 8.** (a) Splitting tensile strength of different concrete mixtures at different ages, (b) Splitting tensile strength variations.

specimen's density (heated in oven for 72 h), and $W_w$ is the specimen's density after immersion in water for 30 min. Fig. 15 shows the variations of the water absorption with increasing values of BOS percentage. As seen, inclusion of nano-silica as substitution of cement led to reduced water absorption, e.g., about 35% reduction was observed, which was due to the micro-filling effect of nano-silica particles. Furthermore, in concrete mixtures with BOS, as the BOS content increased, the water absorption decreased. For the sake of illustration, replacing sand with 25% and 100% BOS, resulted in 46% and 60% reduction in water absorption value, respectively. This owed to the fact that BOS particles were finer than sand, which led to pore refinement of concrete matrix and interfacial transition zone. Also, the results confirmed the findings of the previous studies [76,77]. Palankar et al. [78] reported reduced water absorption in steel slag concrete, which was attributed to the refined structure of the mixture.

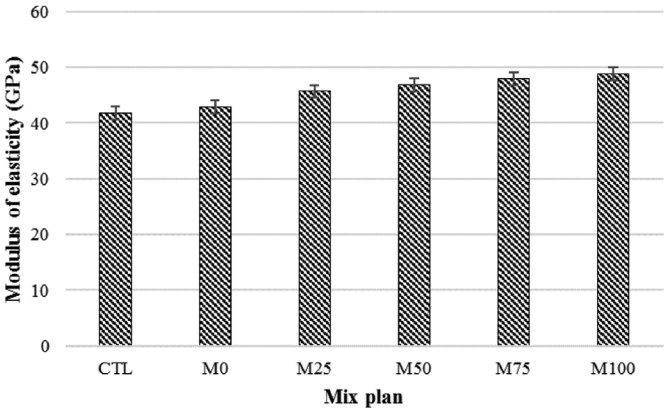


**Fig. 10.** Modulus of elasticity of concrete samples at the age of 28 days.

### 3.5.2. Crack width

Reinforced concrete durability is mainly influenced by the crack

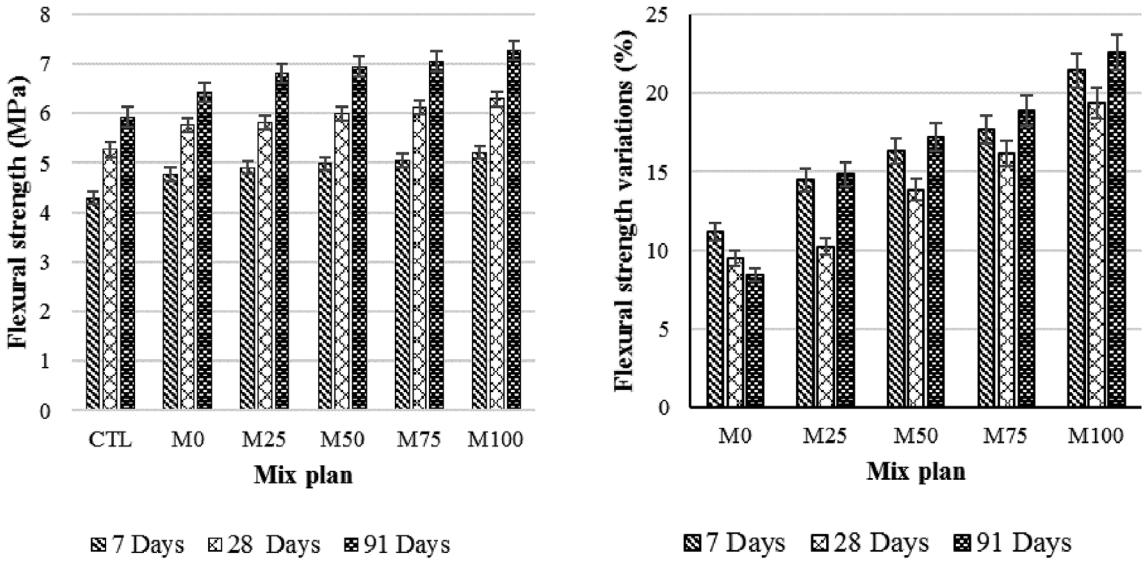


**Fig. 9.** (a) Flexural strength of different concrete mixtures at different ages, (b) Flexural strength variations.

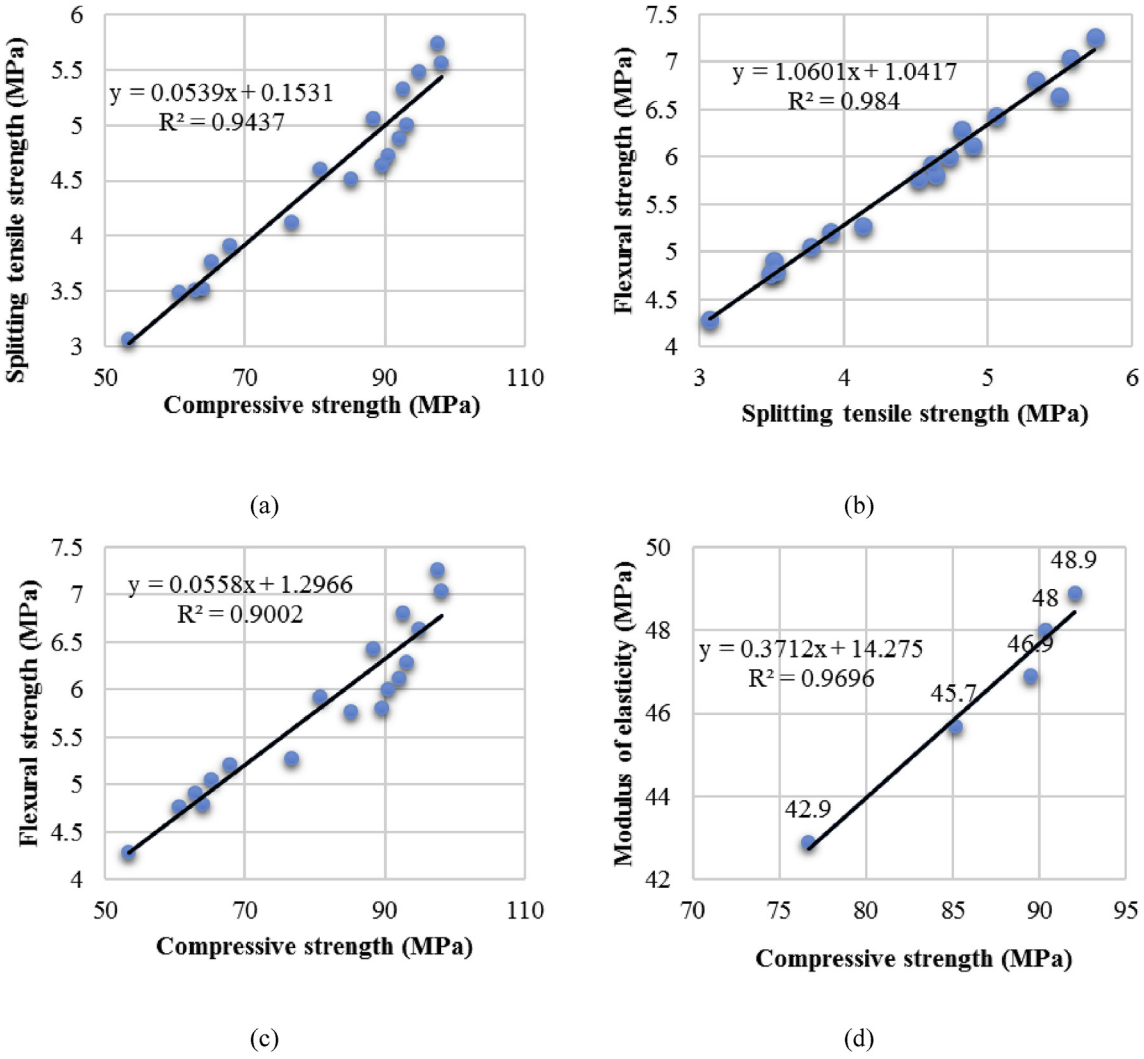


**Fig. 11.** Relationships between different strength properties: (a) relationship between tensile and compressive strength, (b) relationship between flexural and tensile strength, (c) relationship between flexural and compressive strength, (d) relationship between modulus of elasticity and compressive strength.

**Table 3**
Equations proposed by design codes and standards.

| Standard | Modulus of elasticity ($E_c$) (GPa) | Flexural strength ($f_r$) (MPa) | Splitting tensile strength ($f_{st}$) (MPa) |
|---|---|---|---|
| ABA (Iran) | $E_c = 5\sqrt{f'_c}$ | $f_r = 0.60\sqrt{f'_c}$ | – |
| ACI 318–1 [68] | $E_c = 4.73\sqrt{f'_c}$ | $f_r = 0.62\sqrt{f'_c}$ | $f_{st} = 0.53\sqrt{f'_c}$ |
| CSAA23.3–04 [70] | $E_c = 4.5\sqrt{f'_c}$ | $f_r = 0.60\sqrt{f'_c}$ | – |
| EC-04 [71] | $E_c = 22\left(\frac{f_{cm}}{10}\right)^{0.3}$ | $f_r = 0.435 f'^{2/3}_c$ | $f_{st} = 0.3 f'^{2/3}_c$ |
| JSCE-07 [74] | $E_c = 4.7\sqrt{f'_c}$ | – | $f_{st} = 0.44\sqrt{f'_c}$ |
| JCI-08 [72] | $E_c = 6.3 f'^{0.45}_c$ | – | $f_{st} = 0.13 f'^{0.85}_c$ |
| NZS 3101 [75] | $E_c = 3.32\sqrt{f'_c} + 6.9$ | $f_r = 0.60\sqrt{f'_c}$ | $f_{st} = 0.44\sqrt{f'_c}$ |

width. Crack width is an indication of lacking compaction and integrity in mix designs. Different methods are examined to measure crack width such as monitoring the distance between polycarbonate reference points by using a digital calliper [79] or by using a Digital Image Correlation (DIC) technique [80]. In this study, the crack width of cubic samples were determined by using crack width gauge TC410, which is a widely used device for non-destructive evaluation of crack width in tunnels, bridges, and concrete structures. The system is based on taking images from the crack and displays real-time image and calculates the crack width through a powerful processing software [81]. The measuring range of the device is between 0.01 mm and 6.5 mm with the accuracy of 0.02 mm. The results are presented in Fig. 16. As observed, replacing cement with nano-silica reduced the crack width from 0.05 mm (CTL) to 0.03 mm (M0). This owed to the great potential of nano-silica particles to arrest cracks [82]. Conversely, replacing sand with BOS resulted in increase in the crack width, e.g., 0.1 mm increase in crack width of M100 mixture was observed compared to the control sample. This could be ascribed to finer particles of BOS and nano-silica in comparison with natural sand and cement, which increased the water demand of the mixture. Since the water content was kept constant in all mixtures, higher shrinkage and consequent crack formation were expected with increasing values of BOS content. Furthermore, later hydration of BOS particles could be another reason responsible for the increased crack width.

### 3.6. Ultrasonic pulse velocity

Ultrasonic pulse velocity (UPV) test is being widely used as a non-destructive test method in examining the integrity of concrete structures. The UPV test was conducted on 150 × 150 × 150 mm cubic specimens at the ages of 28 days and 91 days using Ultrasonic Concrete Tester 110–240V 50/60Hz 1Ph device. Fig. 17(a) shows the UPV test

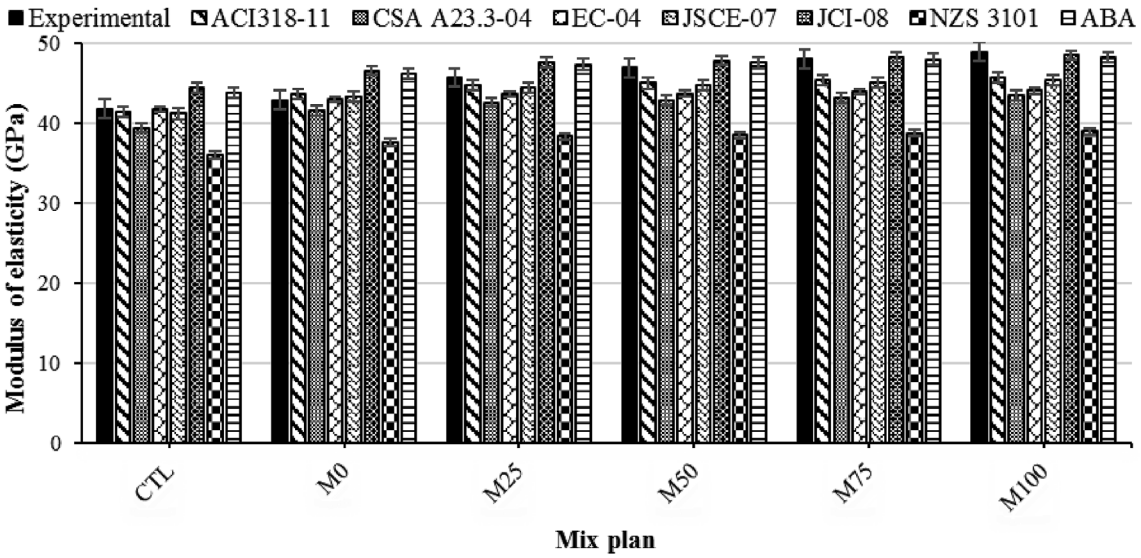


**Fig. 12.** Predicted versus experimental modulus of elasticity.

results for different concrete mixtures at the ages of 28 days and 91 days. As seen, the results adequately satisfied the quality requirements even at high levels of replacement. It was observed that full replacement of natural sand with BOS, led to 27.4% and 29% increase in 28-day and 91-day UPV compared to the control sample, respectively. The increase in pulse velocity was due to reduction in pore size by nano-silica and BOS particles and formation of additional CSH due to pozzolanic reaction between nano-silica and BOS particles and hydration products. Maslehuddin et al. [83] also reported that concrete with steel slag as replacement of aggregates showed higher UPV.

Furthermore, the correlation between UPV and the compressive strength is shown in Fig. 17(b), while Fig. 17(c) demonstrates the linear regression curve fitted to the results. As observed, the results of both tests demonstrated the same trend. A direct relationship was observed between the compressive strength and UPV and the high R-factor value indicates the accuracy of the experimental work.

In addition, the water absorption coefficient is plotted against UPV test results in Fig. 18. As expected, an indirect relationship was observed between the aforementioned properties. In fact, specimens with higher BOS content were less porous, due to pore refinement and additional CSH gel produced by the reaction between nano-silica and $Ca(OH)_2$, which filled the voids of the concrete and as a result, the water absorption of the concrete decreased.

As mentioned before, using high quality fine aggregates is becoming difficult mostly because of environmental and economic limitations. Thus, possible use of industrial by-products as partial replacement of sand has been investigated extensively in the literature. Previous studies suggested various optimum replacement levels of by-products, which are listed in Table 4.

## 4. Conclusions

Based on the findings of the present study, the following conclusions were drawn:

- The incorporation of BOS and nano-silica in concrete led to a reduction in workability. For example, 80% reduction in the slump value was observed when 100% of sand was replaced with BOS.
- The concrete density increased by increasing values of BOS percentages due to the higher specific density of BOS compared to

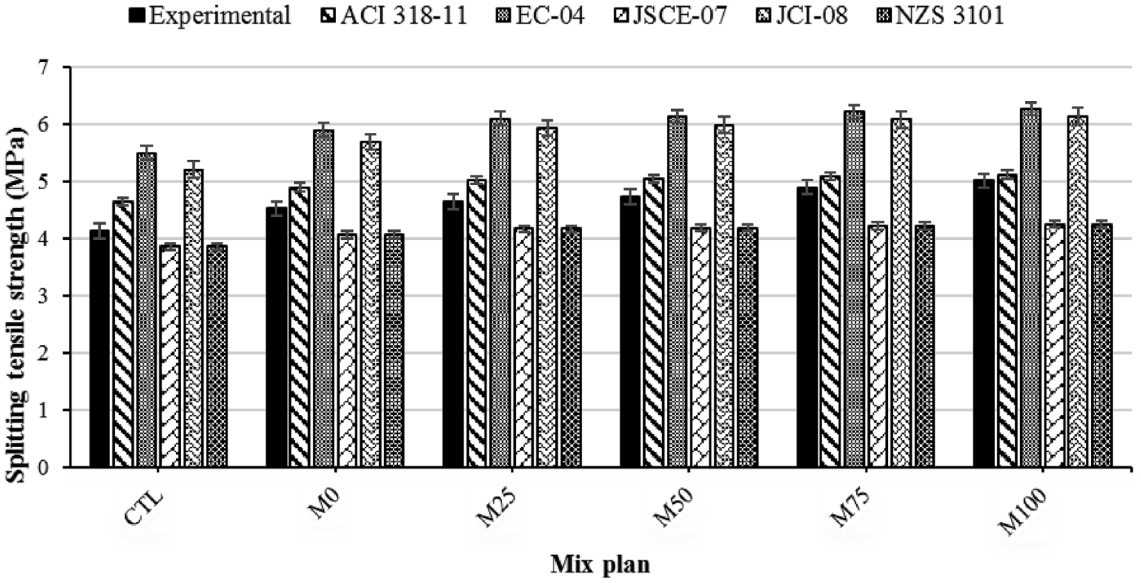


**Fig. 13.** Predicted versus experimental splitting tensile strength.

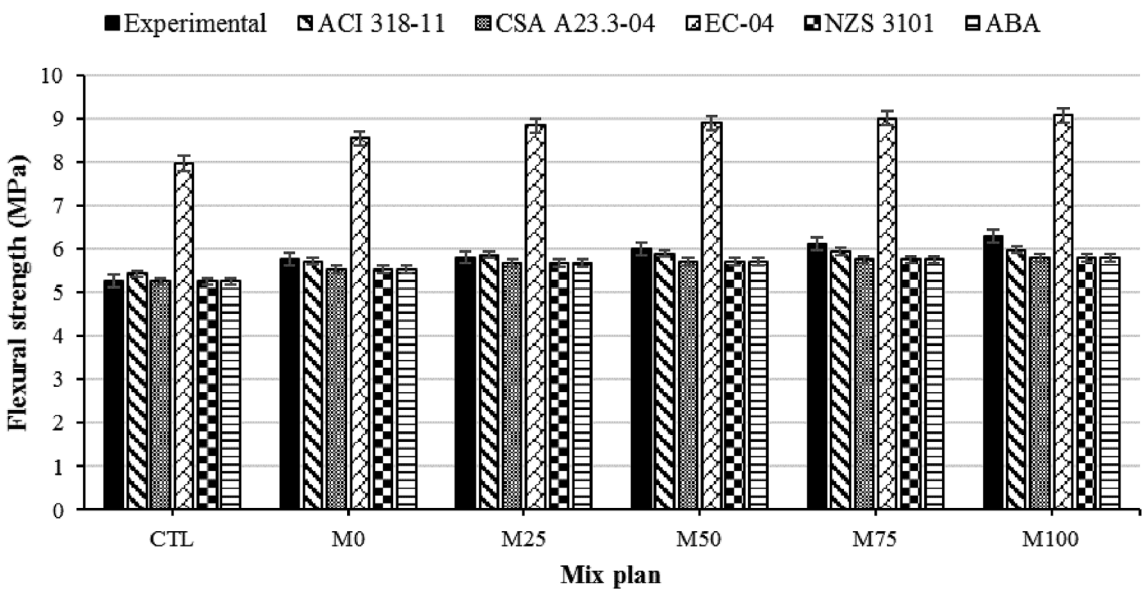


**Fig. 14.** Predicted versus experimental flexural strength.

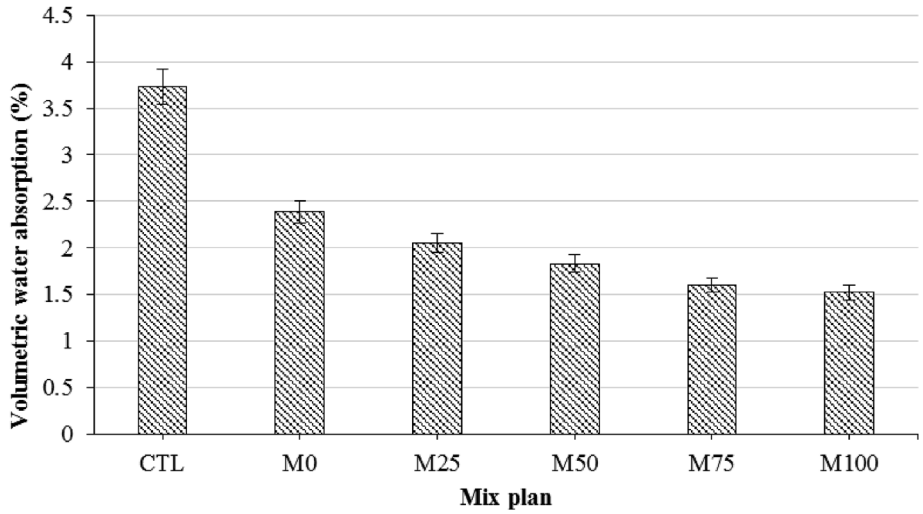


**Fig. 15.** Water absorption of mixtures.

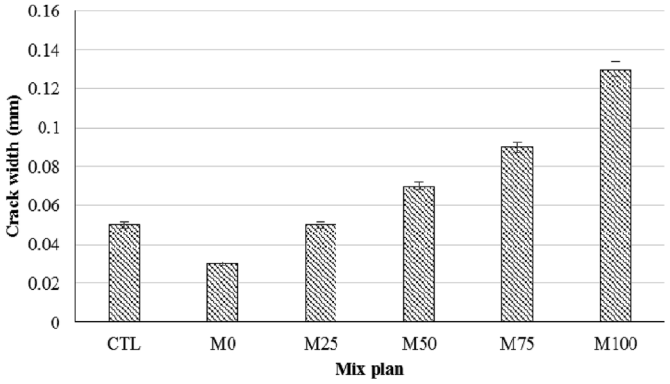


**Fig. 16.** Crack width for different mixtures.

natural sand. For example, by replacing sand with 50% and 100% BOS, the dry density was increased by 6% and 10%, respectively.

- Improvements in strength properties of concrete containing nano-silica and BOS were observed. The strength properties of concrete consistently increased with increasing values of BOS. The maximum increase was observed at 100% replacement of sand with BOS, where 21.4%, 20.3%, and 19.4% increase in 28-day compressive, tensile, and flexural strength were observed, respectively.
- The modulus of elasticity of specimens containing nano-silica and BOS particles was increased as the BOS percentage increased. The increase can be attributed to the micro-filling effect of nano-silica and a series of chemical reactions including hydraulic and pozzolanic reaction between nano-silica and slag and other constituents, which produced additional CSH gel and led to reduced pore size and a denser matrix.
- Water absorption of specimens containing nano-silica and BOS was reduced. This owed to pore refinement by nano-silica and BOS particles. Therefore, the water absorption of the concrete decreased. For example, at 100% replacement of sand with BOS, 60% reduction in water absorption was observed.
- The inclusion of nano-silica reduced the crack width. The nano-silica particles bridged the cracks and prevented further opening of the cracks. However, increasing BOS content resulted in higher crack width due to increased water demand and later hydration of slag.
- In concrete mixtures with nano-silica, it was observed that by

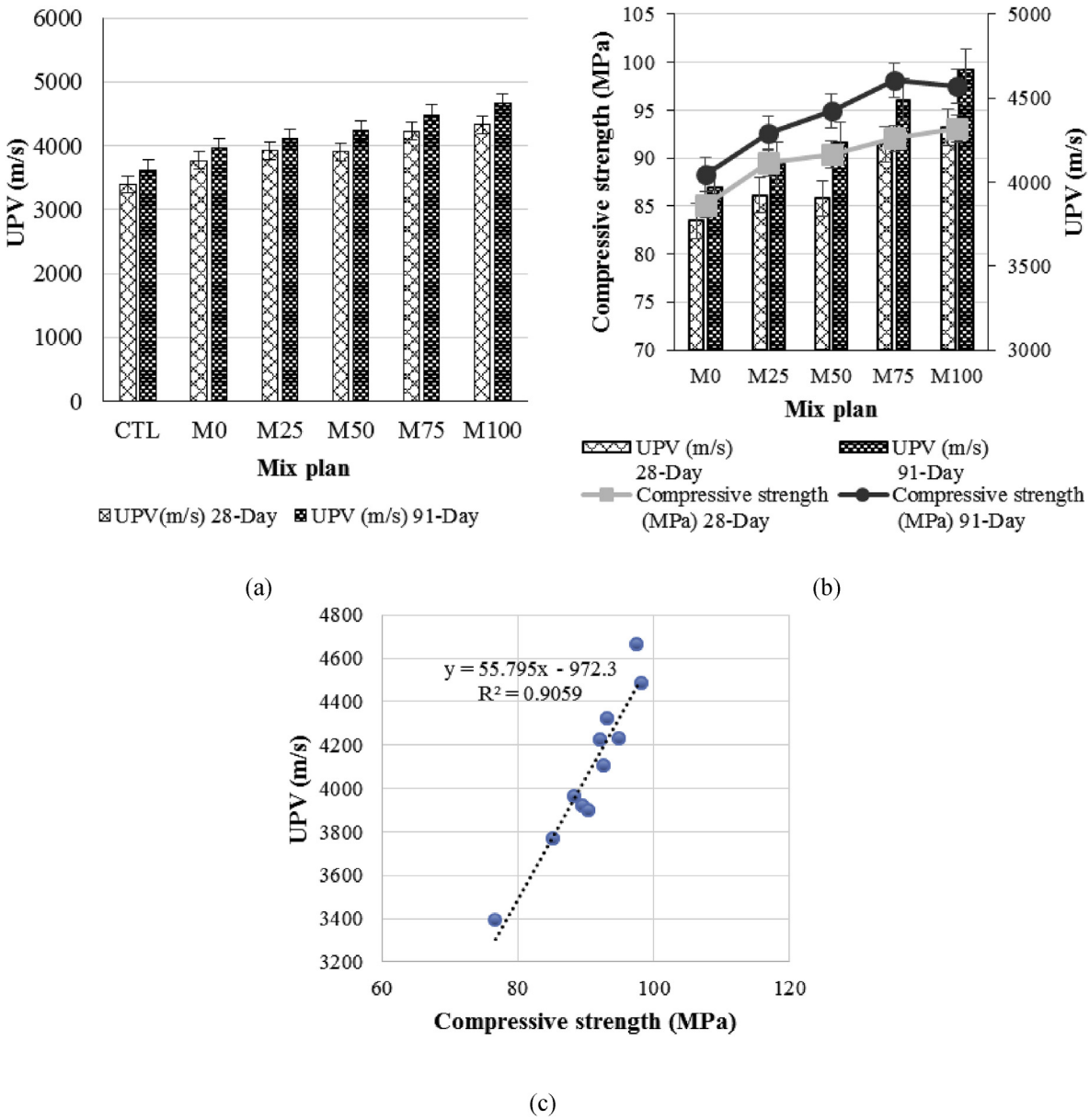


**Fig. 17.** (a) UPV of concrete mixtures at the ages of 28 days and 91 days, (b) Variation of UPV with respect to the compressive strength, (c) Relationship between UPV and compressive strength.

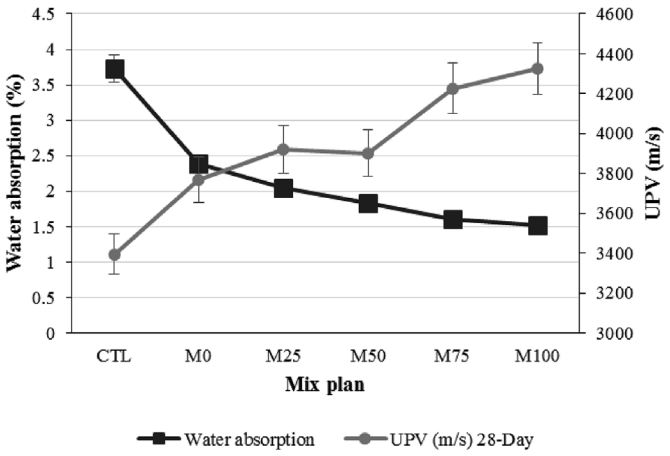


**Fig. 18.** Comparison between water absorption ratio and UPV variations.

increasing BOS content, the pulse velocity increased as well. This was expected, since nano-silica and BOS particles filled the voids and increased the density of concrete.

Based on the findings of this study, it can be concluded that BOS and nano-silica combination reasonably satisfies the strength and durability properties of high strength concrete. It should be noted that each of the industrial wastes presents particular advantages and disadvantages. Further research is required to investigate other potential alternatives to reduce the consumption volume of aggregates in different concrete types.

## Funding

This research did not receive any specific grant from funding agencies in the public, commercial, or not-for-profit sectors.

**Table 4**
Optimum percentage of slag recommended by different studies.

| Type of slag | Type of replacement | Optimum percentage |
|---|---|---|
| Ground granulated blast furnace slag (GGBFS) [84] | Cement | 20% |
| BOF slag [85] | Fine aggregate | 40% |
| Stainless steel slag [86] | Fine and coarse aggregates | 30% |
| Copper Slag | Fine aggregate | 20% |
| Industrial waste slag [87] | Coarse and fine aggregates | 30%–50% |
| Steel slag and crystalized slag [88] | Coarse aggregate | 20% |
| Stainless steel reducing slag (SSRS) [89] | Filler and cement substitution | 20% or less |
| Stainless steel oxidizing slag (SSOS) and stainless steel reducing slag (SSRS) [90] | Fine and coarse aggregates and ordinary Portland Cement | 100% SSOS aggregates and 20% SSRS substituting OPC |
| GGBFS [91] | Cement | 40% |
| Iron slag [65] | Fine aggregate | 40% |
| Ground granulated blast furnace slag (GGBFS) [92] | Cement | 40% slag |
| Granulated blast-furnace slag (GBFS) [93] | Fine aggregate | (100% GBFS) |

## Acknowledgment

The authors would like to thank the staff of the Concrete Laboratory of Civil Engineering Department at Isfahan (Khorasgan) Branch, Islamic Azad University, and also Mobarakeh steel plant and Ardestan cement plant in Isfahan, Iran, for their support and valuable assistance during this study.

## References

[1] J.P. Bravard, M. Goichot, S. Gaillot, Geography of Sand and Gravel Mining in the Lower Mekong River. First Survey and Impact Assessment, EchoGéo 23 (2013).
[2] A.M. Rashad, A preliminary study on the effect of fine aggregate replacement with metakaolin on strength and abrasion resistance of concrete, Constr. Build. Mater. 44 (2013) 487–495, https://doi.org/10.1016/j.conbuildmat.2013.03.038.
[3] H.M. Mehta, P. Kumar, Tools for reducing carbon emissions due to cement consumption, Structure 1 (2009) 11–15.
[4] D.N. Huntzinger, T.D. Eatmon, A life-cycle assessment of Portland cement manufacturing: comparing the traditional process with alternative technologies, J. Clean. Prod. 17 (2009) 668–675, https://doi.org/10.1016/j.jclepro.2008.04.007.
[5] A. Gholampour, T. Ozbakkaloglu, Performance of sustainable concretes containing very high volume Class-F fly ash and ground granulated blast furnace slag, J. Clean. Prod. 162 (2017) 1407–1417, https://doi.org/10.1016/j.jclepro.2017.06.087.
[6] S.A. Zareei, F. Ameri, N. Bahrami, F. Dorostkar, Experimental evaluation of eco-friendly light weight concrete with optimal level of rice husk ash replacement, Civ. Eng. J. 3 (2017) 972–986.
[7] S.A. Zareei, F. Ameri, F. Dorostkar, M. Ahmadi, Rice husk ash as a partial replacement of cement in high strength concrete containing micro silica: evaluating durability and mechanical properties, Case Stud. Constr. Mater. 7 (2017) 73–81.
[8] E.G. Moffatt, M.D.A. Thomas, A. Fahim, Performance of high-volume fly ash concrete in marine environment, Cement Concr. Res. 102 (2017) 127–135.
[9] P. Jiang, L. Jiang, J. Zha, Z. Song, Influence of temperature history on chloride diffusion in high volume fly ash concrete, Constr. Build. Mater. 144 (2017) 677–685.
[10] Y. Hefni, Y.A. El Zaher, M.A. Wahab, Influence of activation of fly ash on the mechanical properties of concrete, Constr. Build. Mater. 172 (2018) 728–734.
[11] N. Tošić, S. Marinković, N. Pecić, I. Ignjatović, J. Dragaš, Long-term behaviour of reinforced beams made with natural or recycled aggregate concrete and high-volume fly ash concrete, Constr. Build. Mater. 176 (2018) 344–358.
[12] P. Shoaei, S. Zolfaghary, N. Jafari, M. Dehestani, M. Hejazi, Investigation of adding cement kiln dust (CKD) in ordinary and lightweight concrete, Adv. Concr. Constr. 5 (2017) 101–115.
[13] S.A. Zareei, F. Ameri, F. Dorostkar, S. Shiran, Partial replacement of limestone and silica powder as a substitution of cement in lightweight Aggregate concrete, Civ. Eng. J. 3 (2017) 727–740.
[14] S.A. Zareei, F. Ameri, N. Bahrami, Microstructure, strength, and durability of eco-friendly concretes containing sugarcane bagasse ash, Constr. Build. Mater. 184 (2018) 258–268, https://doi.org/10.1016/J.CONBUILDMAT.2018.06.153.
[15] E. Rahmani, M. Dehestani, M.H.A. Beygi, H. Allahyari, I.M. Nikbin, On the mechanical properties of concrete containing waste PET particles, Constr. Build. Mater. 47 (2013) 1302–1308.
[16] L. Zhang, K.M. Liew, A.O. Sojobi, Green concrete: prospects and challenges, Constr. Build. Mater. 156 (2017) 1063–1095.
[17] A. Rashad, Cementitious materials and agricultural wastes as natural fine aggregate replacement in conventional mortar and concrete, J. Build. Eng. 5 (2016) 119–141.
[18] S.P. Palanisamy, G. Maheswaran, M.G.L. Annaamalai, P. Vennila, Steel slag to improve the high strength of concrete, Int. J. Chem. Res. 7 (2015).
[19] A.E.A.E.M. Behiry, Evaluation of steel slag and crushed limestone mixtures as subbase material in flexible pavement, Ain Shams Eng. J. 4 (2013) 43–53, https://doi.org/10.1016/j.asej.2012.07.006.
[20] E. Furlani, G. Tonello, S. Maschio, Recycling of steel slag and glass cullet from energy saving lamps by fast firing production of ceramics, Waste Manag. 30 (2010) 1714–1719, https://doi.org/10.1016/j.wasman.2010.03.030.
[21] P.H. J, Influence of micro silica and steel slag on properties of high strength concrete, Int. J. Adv. Res. Eng. Sci. Technol. 3 (2016).
[22] H. Motz, J. Geiseler, Products of steel slags an opportunity to save natural resources, Waste Manag. 21 (2001) 285–293, https://doi.org/10.1016/S0956-053X(00)00102-1.
[23] X.Z. HOU, Gui-hua, W.A.N.G. Zhan-hong, Difference of grindablity and cementions performance activity among minerals in steel slag [J], J. Yancheng Inst. Technol. (Natural Sci. Ed. (2011) 3.
[24] G. Wang, Y. Wang, Z. Gao, Use of steel slag as a granular material: volume expansion prediction and usability criteria, J. Hazard Mater. 184 (2010) 555–560, https://doi.org/10.1016/j.jhazmat.2010.08.071.
[25] M. Maslehuddin, A.M. Sharif, M. Shameem, M. Ibrahim, M.S. Barry, Comparison of properties of steel slag and crushed limestone aggregate concretes, Constr. Build. Mater. 17 (2003) 105–112.
[26] W. GUO, D. CANG, Z. YANG, Y. LI, C. WEI, Study on preparation of glass-ceramics from reduced slag after iron melt-reduction, Bull. Chinese Ceram. Soc. 5 (2011) 51.
[27] V. Subathra Devi, B.K. Gnanavel, Properties of concrete manufactured using steel slag, Procedia Eng. 2014, pp. 95–104, , https://doi.org/10.1016/j.proeng.2014.12.229.
[28] C.B. Echeta, E.E. Ikponmwosa, A.O. Fadipe, Effect of partial replacement of granite with washed gravel on the characteristic strength and workability of concrete, ARPN J. Eng. Appl. Sci. 8 (2013).
[29] P.S. Kothai, R. Malathy, Utilization of steel slag in concrete as a partial replacement material for fine aggregates, Int. J. Innov. Res. Sci. Eng. Technol. 3 (2014).
[30] R. Manjunath, M.C. Narasimhan, An experimental investigation on self-compacting alkali activated slag concrete mixes, J. Build. Eng. 17 (2018) 1–12.
[31] A.C. Aydın, V.J. Nasl, T. Kotan, The synergic influence of nano-silica and carbon nano tube on self-compacting concrete, J. Build. Eng. 20 (2018) 467–475.
[32] O.A. Naniz, M. Mazloom, Effects of colloidal nano-silica on fresh and hardened properties of self-compacting lightweight concrete, J. Build. Eng. 20 (2018) 400–410.
[33] B.S. Mohammed, M. Adamu, Mechanical performance of roller compacted concrete pavement containing crumb rubber and nano silica, Constr. Build. Mater. 159 (2018) 234–251.
[34] AASHTO, Soundness of aggregate by use of sodium sulfate or magnesium sulfate, T 104, ASTM International, West Conshohocken, PA, 2011.
[35] A.T. 96, Standard method of test for resistance to degradation of small-size coarse aggregate by abrasion and impact in the Los Angeles machine (ASTM C 131-01), Am. Assoc. State Highw. Transp. Off. (2002).
[36] ASTM D 5821-13, Standard Test Method for determining the percentage of fractured particles in coarse aggregate, Annu. B. Am. Soc. Test. Mater. ASTM Stand. (2014) 1–6, https://doi.org/10.1520/D5821-13.2.
[37] R. Yu, P. Tang, P. Spiesz, H.J.H. Brouwers, A study of multiple effects of nano-silica and hybrid fibres on the properties of Ultra-High Performance Fibre Reinforced Concrete (UHPFRC) incorporating waste bottom ash (WBA), Constr. Build. Mater. 60 (2014) 98–110, https://doi.org/10.1016/j.conbuildmat.2014.02.059.
[38] A.C./C.- 16e1, Standard Specification for Concrete Aggregates, (2012).
[39] F. Shaikh, V. Chavda, N. Minhaj, H.S. Arel, Effect of mixing methods of nano silica on properties of recycled aggregate concrete, Struct. Concr. 19 (2018) 387–399.
[40] S. Fallah, M. Nematzadeh, Mechanical properties and durability of high-strength concrete containing macro-polymeric and polypropylene fibers with nano-silica and silica fume, Constr. Build. Mater. 132 (2017) 170–187.
[41] M. Amin, K. Abu el-Hassan, Effect of using different types of nano materials on mechanical properties of high strength concrete, Constr. Build. Mater. 80 (2015) 116–124.
[42] P. Sharmila, G. Dhinakaran, Compressive strength, porosity and sorptivity of ultra fine slag based high strength concrete, Constr. Build. Mater. 120 (2016) 48–53.
[43] Y. Yang, R. Sato, K. Kawai, Autogenous shrinkage of high-strength concrete containing silica fume under drying at early ages, Cement Concr. Res. 35 (2005) 449–456.
[44] M. Aslam, P. Shafigh, M.A. Nomeli, M.Z. Jumaat, Manufacturing of high-strength lightweight aggregate concrete using blended coarse lightweight aggregates, J.

Build. Eng. 13 (2017) 53–62.
[45] I. 10086, Specification for Moulds for Use in Tests of Cement and Concrete, (2001).
[46] ASTM C143/C143M -12, Standard Test Method for Slump of Hydraulic Cement Concrete, American Society for Testing and Materials, 2007.
[47] A. C138/C138M-14, Standard Test Method for Density (Unit Weight), Yield, and Air Content (Gravimetric) of Concrete, American Society for Testing and Materials, 2016.
[48] A. C642-13, Standard Test Method for Density, Absorption, and Voids in Hardened Concrete, American Society for Testing and Materials, 2013.
[49] A.D.- 14, Standard Test Method for Determining the Relative Density (Specific Gravity) and Absorption of Fine Aggregates Using Infrared, (2014).
[50] ASTM C39/C39M-16, Standard Test Method for Compressive Strength of Cylindrical Concrete Specimens, ASTM International West, Conshohocken, PA, 2016.
[51] A.S.T.M. Norma, C496/C496M-11, Standard Test Method for Splitting Tensile Strength of Cylindrical Concrete Specimens, (2004), pp. 469–490.
[52] ASTM C78/C78M-16, Standard Test Method for Flexural Strength of Concrete (Using Simple Beam with Third-Point Loading), ASTM International West, Conshohocken, PA, 2016.
[53] ASTM C469/C469M-14, Standard test method for static modulus of elasticity and Poisson's ratio of concrete in compression, ASTM International West Conshohocken, PA, 2014 http://portales.puj.edu.co/wjfajardo/mecanica de solidos/laboratorios/astm/C469.pdf.
[54] A.E.- 15, Standard Test Method for Measurement of Initiation Toughness in Surface Cracks under Tension and Bending, (2015).
[55] C. ASTM, Standard Test Method for Pulse Velocity through Concrete, ASTM International, West Conshohocken, PA, 2009.
[56] H.K. Kim, E.A. Hwang, H.K. Lee, Impacts of metakaolin on lightweight concrete by type of fine aggregate, Constr. Build. Mater. 36 (2012) 719–726.
[57] C. Pellegrino, V. Gaddo, Mechanical and durability characteristics of concrete containing EAF slag as aggregate, Cement Concr. Compos. 31 (2009) 663–671.
[58] J.T. San-José, I. Vegas, I. Arribas, I. Marcos, The performance of steel-making slag concretes in the hardened state, Mater. Des. 60 (2014) 612–619.
[59] Y.-N. Sheen, H.-Y. Wang, T.-H. Sun, Properties of green concrete containing stainless steel oxidizing slag resource materials, Constr. Build. Mater. 50 (2014) 22–27.
[60] I. Arribas, I. Vegas, J.T. San-Jose, J.M. Manso, Durability studies on steelmaking slag concretes, Mater. Des. 63 (2014) 168–176.
[61] H. Bnci, M.Y. Durgun, T. Rzaolu, M. Koluçolak, Investigation of durability properties of concrete pipes incorporating blast furnace slag and ground basaltic pumice as fine aggregates, Sci. Iran. 19 (2012) 366–372, https://doi.org/10.1016/j.scient.2012.04.007.
[62] H. Qasrawi, The use of steel slag aggregate to enhance the mechanical properties of recycled aggregate concrete and retain the environment, Constr. Build. Mater. 54 (2014) 298–304.
[63] Sidney Mindess, J Francis Young, David Darwin, Mineral Admixture and Blended Cements, Concrete, (2003).
[64] R. Sharma, P.P. Bansal, Use of different forms of waste plastic in concrete–a review, J. Clean. Prod. 112 (2016) 473–482.
[65] G. Singh, R. Siddique, Strength properties and micro-structural analysis of self-compacting concrete made with iron slag as partial replacement of fine aggregates, Constr. Build. Mater. 127 (2016) 144–152, https://doi.org/10.1016/j.conbuildmat.2016.09.154.
[66] X. Feng, E.J. Garboczi, D.P. Bentz, P.E. Stutzman, T.O. Mason, Estimation of the degree of hydration of blended cement pastes by a scanning electron microscope point-counting procedure, Cement Concr. Res. 34 (2004) 1787–1793, https://doi.org/10.1016/j.cemconres.2004.01.014.
[67] M. Etxeberria, C. Pacheco, J.M. Meneses, I. Berridi, Properties of concrete using metallurgical industrial by-products as aggregates, Constr. Build. Mater. 24 (2010) 1594–1600, https://doi.org/10.1016/j.conbuildmat.2010.02.034.
[68] A. 318-11, ACI committee, Am. Concr. Inst. Int. Organ, Stand. Build. Code Requir. Struct. Concr. Comment. (2011).
[69] A 3600, Concrete structures, Stand. Aust (2009) 105–109.
[70] CSA, Design of concrete structures, Can. Stand. Assoc. (2004).
[71] E. 04, B.S. Institution, Eurocode 2: Design of Concrete Structures: Part 1–1, General Rules and Rules for Buildings, 2004.
[72] J.C.I, Guidelines for Control of Cracking of Mass Concrete, Japan Concr. Inst., 2008.
[73] N. Standard, Concrete structures standard: NZS 3101 (2006).
[74] J.S.C.E, Engineers, Standard Specification for Concrete Structure, (2007).
[75] NZ, Concrete Structures Standard: NZS 3101 (2006).
[76] A.M. Rashad, A brief review on blast-furnace slag and copper slag as fine aggregate in mortar and concrete based on portland cement, Rev. Adv. Mater. Sci. 44 (2016).
[77] A. Aghaeipour, M. Madhkhan, Effect of ground granulated blast furnace slag (GGBFS) on RCCP durability, Constr. Build. Mater. 141 (2017) 533–541.
[78] N. Palankar, A.U.R. Shankar, B.M. Mithun, Durability studies on eco-friendly concrete mixes incorporating steel slag as coarse aggregates, J. Clean. Prod. 129 (2016) 437–448.
[79] F. Pedrosa, C. Andrade, Corrosion induced cracking: effect of different corrosion rates on crack width evolution, Constr. Build. Mater. 133 (2017) 525–533.
[80] C. Barris, L. Torres, I. Vilanova, C. Miàs, M. Llorens, Experimental study on crack width and crack spacing for Glass-FRP reinforced concrete beams, Eng. Struct. 131 (2017) 231–242.
[81] Crack Width Gauge,Crack Width Gauge TC410,Concrete Testing Gauge,Beijing times of the peak Tech, (n.d.).http://www.tgindt.com/products_detail/productId=83.html (accessed July 14, 2018).
[82] P. Jaishankar, K.S.R. Mohan, Influence of nano particles in high performance concrete (HPC), Int. J. Chem. Res. 8 (2015) 278–284.
[83] M. Maslehuddin, A.M. Sharif, M. Shameem, M. Ibrahim, M.S. Barry, Comparison of properties of steel slag and crushed limestone aggregate concretes, Constr. Build. Mater. 17 (2003) 105–112.
[84] R. Siddique, D. Kaur, Properties of concrete containing ground granulated blast furnace slag (GGBFS) at elevated temperatures, J. Adv. Res. 3 (2012) 45–51, https://doi.org/10.1016/j.jare.2011.03.004.
[85] Y.C. Ding, T.W. Cheng, P.C. Liu, W.H. Lee, Study on the treatment of BOF slag to replace fine aggregate in concrete, Constr. Build. Mater. 146 (2017) 644–651, https://doi.org/10.1016/j.conbuildmat.2017.04.164.
[86] Y. Sheen, L.-J. Huang, T.-H. Sun, D.-H. Le, Engineering properties of self-compacting concrete containing stainless steel slags, Procedia Eng 142 (2016) 79–86, https://doi.org/10.1016/j.proeng.2016.02.016.
[87] M. Nadeem, Utilization of industrial waste slag as aggregate in concrete applications by adopting Taguchi's approach for optimization, Open J. Civ. Eng. 2 (2012) 96–105, https://doi.org/10.4236/ojce.2012.23015.
[88] Y. Biskri, D. Achoura, N. Chelghoum, M. Mouret, Mechanical and durability characteristics of High Performance Concrete containing steel slag and crystalized slag as aggregates, Constr. Build. Mater. 150 (2017) 167–178, https://doi.org/10.1016/j.conbuildmat.2017.05.083.
[89] Y.N. Sheen, D.H. Le, T.H. Sun, Greener self-compacting concrete using stainless steel reducing slag, Constr. Build. Mater. 82 (2015) 341–350, https://doi.org/10.1016/j.conbuildmat.2015.02.081.
[90] Y.N. Sheen, D.H. Le, T.H. Sun, Innovative usages of stainless steel slags in developing self-compacting concrete, Constr. Build. Mater. 101 (2015) 268–276, https://doi.org/10.1016/j.conbuildmat.2015.10.079.
[91] A.M. Shariq, Mohd, Jagdish Prasad, Studies in ultrasonic pulse velocity of concrete containing GGBFS, Constr. Build. Mater. 40 (2013) 944–950.
[92] M.M. Aghaeipour, Arash, Effect of ground granulated blast furnace slag (GGBFS) on RCCP durability, Constr. Build. Mater. 141 (2017) 533–541.
[93] A.M. Rashad, D.M. Sadek, H.A. Hassan, An investigation on blast-furnace stag as fine aggregate in alkali-activated slag mortars subjected to elevated temperatures, J. Clean. Prod. 112 (2016) 1086–1096, https://doi.org/10.1016/j.jclepro.2015.07.127.